

# PCCP

Accepted Manuscript



This is an *Accepted Manuscript*, which has been through the Royal Society of Chemistry peer review process and has been accepted for publication.

*Accepted Manuscripts* are published online shortly after acceptance, before technical editing, formatting and proof reading. Using this free service, authors can make their results available to the community, in citable form, before we publish the edited article. We will replace this *Accepted Manuscript* with the edited and formatted *Advance Article* as soon as it is available.

You can find more information about *Accepted Manuscripts* in the [Information for Authors](#).

Please note that technical editing may introduce minor changes to the text and/or graphics, which may alter content. The journal's standard [Terms & Conditions](#) and the [Ethical guidelines](#) still apply. In no event shall the Royal Society of Chemistry be held responsible for any errors or omissions in this *Accepted Manuscript* or any consequences arising from the use of any information it contains.

Cite this: DOI: 10.1039/c0xx00000x

www.rsc.org/xxxxxx

ARTICLE TYPE

## Modeling of catalytically active metal complex species and intermediates in reactions of organic halides electroreduction

Anton S. Lytvynenko,<sup>a\*</sup> Sergey V. Kolotilov,<sup>a</sup> Mikhail A. Kiskin,<sup>b</sup> Igor L. Eremenko,<sup>b</sup> Vladimir M. Novotortsev<sup>b</sup>

<sup>5</sup> Received (in XXX, XXX) Xth XXXXXXXXX 20XX, Accepted Xth XXXXXXXXX 20XX

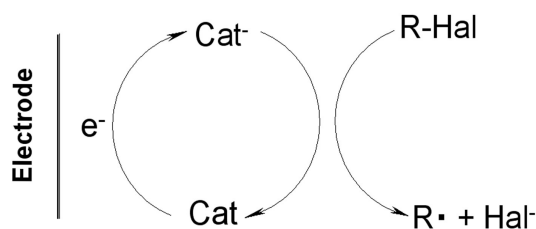
DOI: 10.1039/b000000x

The results of quantum chemical modeling of organic and metal-containing intermediates which occur in the reactions of electrocatalytic dehalogenation of organic chlorides are presented. Modeling of processes which take place on consequent steps of electrochemical reduction of the representatives of C<sub>1</sub> and C<sub>2</sub> chlorides – CHCl<sub>3</sub> and freon R113 (1,1,2-trifluoro-1,2,2-trichloroethane) – was carried out by density functional theory (DFT) and second-order Møller–Plesset perturbation theory (MP2). It was found that taking solvation into account using implicit solvent model (conductor-like screening model, COSMO) or considering explicit solvent molecules gave similar results. In addition to modeling of raw non-catalytic dehalogenation, processes with a number of complexes and their reduced forms, some of which were catalytically active, were investigated by DFT. Complexes M(L1)<sub>2</sub> (M = Fe, Co, Ni, Cu, Zn, L1H = Schiff base from 2-pyridinecarbaldehyde and hydrazide of 4-pyridinecarboxylic acid), Ni(L2) (H<sub>2</sub>L2 is Schiff base from salicylaldehyde and 1,2-ethylenediamine, known as Salen) and Co(L3)<sub>2</sub>Cl<sub>2</sub>, representing a fragment of redox-active coordination polymer [Co(L3)Cl<sub>2</sub>]<sub>n</sub> (L3 is dithioamide of 1,3-benzenedicarboxylic acid), were considered. Gradual changes of electronic structure in a series of compounds M(L1)<sub>2</sub> were observed, correlations between [M(L1)<sub>2</sub>]<sup>0</sup> spin-up and spin-down LUMO energies and relative energies of the corresponding high-spin and low-spin reduced forms as well as the shape of the orbitals were proposed. These results allow to elaborate prompts for DFT-based estimation of the nature of the redox-transitions. No specific covalent interactions between [M(L1)<sub>2</sub>]<sup>-</sup> and R113 molecule (M = Fe, Co, Ni, Zn) were found, which indicates that M(L1)<sub>2</sub> electrocatalysts act rather like electron transfer mediators via outer shell electron transfer. Relaxed surface scan of the adducts {M(L1)<sub>2</sub>·R113}<sup>-</sup> (M = Ni or Co) versus distance between chlorine atom leaving at reduction and the corresponding carbon atom showed energy barrier of electron transfer (the first stage of R113 catalytic reduction), while DFT optimization of {Ni(L2)·R113}<sup>-</sup> adduct showed barrier-less decomposition. The difference between stabilities of {Ni(L1)<sub>2</sub>·R113}<sup>-</sup> and {Ni(L2)·R113}<sup>-</sup> adducts correlates with the difference between catalytic activity of Ni(L1)<sub>2</sub> and Ni(L2) in electrochemical reduction of R113.

## Introduction

During recent decades many efforts were devoted to studies of electrocatalytic reactions, catalyzed by complexes of 3d metals.<sup>1-6</sup> In particular, reactions of organic halides reductive dehalogenation catalyzed by metal complexes have been attracting attention<sup>7-9</sup> because they allow to obtain valuable organic compounds. For example, freons conversion can be used for synthesis of many fluorine-containing compounds, including halogenated olefins,<sup>7</sup> carboxylic or sulfonic acids, aldehydes, ketones.<sup>8,10,11</sup> Metal-catalyzed dehalogenation of organic compounds is also considered as a method for pollutants elimination from water.<sup>12</sup>

The catalytic action of metal complex in reductive process involves the stage of electron acceptance by the catalyst (catalyst reduction) followed by substrate reduction by the reduced form of the catalyst (Scheme 1). The catalyst can participate in several consequent electron transfer acts, which gives rise to growth of the cathodic current. In the majority of cases one-electron reduction of substrate initiates a cascade of reactions, and one of the products can accept one more electron (leading to two-electron reduction in total).<sup>13</sup> Depending on the structure of the catalyst, electrocatalytic reduction of organic compounds can involve coordination of substrate (or its fragment) to metal center<sup>7,14,15</sup> or out-of-sphere electron transfer without substrate binding.<sup>16</sup> Studies of electronic structure of reduced forms of complexes, which show electrocatalytic activity, are important for understanding of the mechanism of such catalytic processes. It should be noted that information about electronic structure of such species can be obtained experimentally<sup>17</sup>. However, direct characterization of reduced forms of metal complexes (*i.e.* their isolation and study by "usual" methods) is not trivial task because of their extreme air-sensitivity and/or low stability, and the attempts to perform preparative chemical or electrochemical reduction give no guarantee, that the isolated form is the most stable form (in contrast to, for example, less soluble compound or the product of multi-step transformations).



**Scheme 1** Catalytic action of redox-active compound in the first stage of reductive dehalogenation of organic halides.

Recently we reported electrocatalytic reduction of freon R113 ( $\text{CF}_2\text{Cl}-\text{CFCl}_2$ ) and  $\text{CHCl}_3$  by similar isostructural complexes  $\text{M}(\text{L}1)_2$  (where  $\text{M} = \text{Ni}, \text{Co}, \text{Fe}, \text{Zn}$ ; L1H is Schiff base from hydrazide of 4-pyridinecarboxylic acid and 2-pyridinecarbaldehyde, Fig. 1).<sup>18,19</sup> It was also shown that electrochemical activity of  $\text{M}(\text{L}1)_2$  ( $\text{M} = \text{Ni}, \text{Co}$ ) preserved upon incorporation of these species as bridging units into porous coordination polymers  $\{\text{Fe}_2\text{M}'\text{O}(\text{Piv})_6\}_n\{\text{M}(\text{L}1)_2\}_{1.5}$  ( $\text{M} = \text{Ni}^{\text{II}}, \text{M}' = \text{Co}^{\text{II}}, \text{M} = \text{Co}^{\text{II}}, \text{M}' = \text{Ni}^{\text{II}}$ ).

In order to get better understanding of the electron transfer

pathway in reactions of electrocatalytic reduction of organic halides (Scheme 1) and to reveal intermediates which participate in these reactions, we performed quantum-chemical modeling of species, which can form in the result of reduction of two halides and seven metal complexes, as well as the adducts of some species with solvent (DMF) or adducts "reduced catalyst + halide". The aim of this study was to elucidate the processes, which can occur upon electrocatalytic reduction of organic halides, in particular: (i) to determine stable intermediates which can form upon electron acceptance by organic halide and to reveal pathway of such anions decomposition; (ii) to reveal the place of "additional" electron localization in reduced complexes (reduced forms of the catalysts); and (iii) to model evolution of adducts of such reduced catalyst and organic halide in order to evaluate electron transfer barrier (if any).

In the present paper we report the results of DFT and MP2 modeling of reduction of  $\text{CHCl}_3$  and freon R113, which to certain extent can be considered as the representatives of  $\text{C}_1$  and  $\text{C}_2$  chlorides. It was shown that primary radical anion which formed upon halide molecule reduction was unstable in both cases (R113 and  $\text{CHCl}_3$ ) and decomposed, eliminating chloride anion. Further reduction of the formed radicals led to stable anion  $\text{CHCl}_2^-$  in the case of  $\text{CHCl}_3$  or to elimination of the second  $\text{Cl}^-$  and formation of  $\text{CF}_2=\text{CFCl}$  in the case of R113. Modeling of species was carried out in implicit solvent or with explicit solvent, but no significant interactions with any molecule or anion were found, as well as no substantial influence of the explicit solvent on the results of the modeling was observed. Also, we carried out DFT modeling of a series of  $[\text{M}(\text{L}1)_2]^0$  ( $\text{M} = \text{Fe}, \text{Co}, \text{Ni}, \text{Cu}, \text{Zn}$ ) complexes and their reduced forms. It was found that these complexes exhibited different nature of electrochemical redox-processes  $[\text{M}(\text{L}1)_2]^0/[\text{M}(\text{L}1)_2]^-$ , gradually changing from mainly ligand-centered in  $[\text{Zn}(\text{L}1)_2]$  and  $[\text{Ni}(\text{L}1)_2]$  to mainly metal-centered in  $[\text{Cu}(\text{L}1)_2]$ . It was found that  $[\text{M}(\text{L}1)_2]^-$  species (except  $[\text{Zn}(\text{L}1)_2]^-$ ) could exist in two pseudodegenerate spin states, which were studied in details for  $\text{M} = \text{Ni}$  or  $\text{Co}$ . Energy differences between these forms were small enough to allow both states to be thermally populated. The difference between the energies of calculated spin-up (close for all complexes in the series) and spin-down LUMO (the energy of the latter is slightly higher for  $[\text{Ni}(\text{L}1)_2]$  than spin-up one and decreases in the series  $[\text{Ni}(\text{L}1)_2] > [\text{Fe}(\text{L}1)_2] > [\text{Co}(\text{L}1)_2] > [\text{Cu}(\text{L}1)_2]$ ) correlated with the relative energies of low-spin and high-spin states; it also correlated with experimental  $E_{1/2}$  potentials of the appropriate redox-transitions, as well as with the nature (shape and Mulliken population on the metal ion) of the spin-down LUMO orbital. To check if such situation is typical or not we modeled reduced form of  $\text{Ni}(\text{L}2)$  complex by DFT; this compound was chosen due to its well-known electrocatalytic activity<sup>20</sup> (L2 is Schiff base from salicylaldehyde and 1,2-ethylenediamine, known as Salen, Fig. 1). In contrast to  $\text{M}(\text{L}1)_2$  complexes, an "additional" electron in reduced form of  $\text{Ni}(\text{L}2)$  was localized on orbital of metal. Then, DFT modeling of reduced form of  $\text{Co}(\text{L}3)_2\text{Cl}_2$  was carried out in order to see the influence of donor atom (S compared to N and O) on localization of additional electron in reduced compounds (L3 is dithioamide of 1,3-benzenedicarboxylic acid, Fig. 1). A species  $\text{Co}(\text{L}3)_2\text{Cl}_2$  is a fragment of coordination polymer  $[\text{Co}(\text{L}3)\text{Cl}_2]_n$ , previously reported by us,<sup>21</sup> it was chosen, besides the presence

Cite this: DOI: 10.1039/c0xx00000x

www.rsc.org/xxxxxx

## ARTICLE TYPE

of S atoms in coordination sphere, due to its redox-activity (which was checked in separate experiment, Supporting Information).

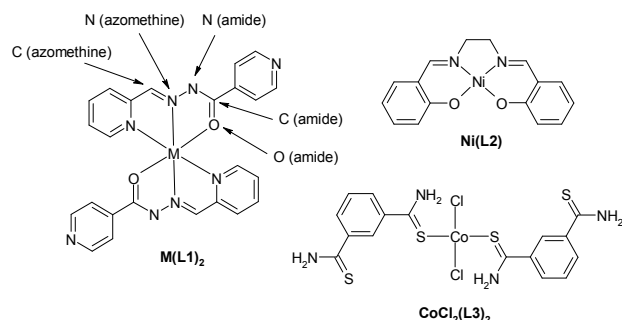


**Fig. 1** Formulae of complexes  $M(L1)_2$  ( $M^II = Ni, Co$ ),  $Ni(L2)$  and  $CoCl_2(L3)_2$ , considered in this study.  $CoCl_2(L3)_2$  species is a fragment of reported coordination polymer  $[Co(L3)Cl_2]_n$ .<sup>21</sup>

Finally, examination of electron transfer from reduced catalyst to halide was carried out. DFT optimization of adducts  $\{[M(L1)_2] \cdot R113\}^-$  ( $M = Ni, Fe, Co, Zn$ ) showed that there were no specific covalent interactions between  $[M(L1)_2]^-$  and R113 molecule (the electrocatalysts act like electron transfer mediators via outer shell electron transfer). Relaxed surface scan (RSS) of these adducts for  $M = Ni$  or  $Co$  revealed energy barrier of electron transfer to halide. In contrast, DFT optimization of  $\{[M(L2)] \cdot R113\}^-$  species led to its barrier-less decomposition.

## Results and discussion

### Modeling of halides reduction

Electrochemical dehalogenation of  $CHCl_3$  and freon R113 ( $CF_2Cl-CFCl_2$ ) in DMF with tetraalkylammonium background electrolytes on electrochemically inert electrodes mostly led to  $CH_2Cl_2$  and  $CF_2=CFCl$ , respectively.<sup>22,23</sup> Studies of exact mechanisms of electrochemical dehalogenation reactions were carried out,<sup>13</sup> which showed that at first a molecule of an organic halide accepted an electron forming the radical anion (rate-determining step) which was involved in a set of degradation reactions depending on the structure of the radical and the conditions of the process. However, processes that occur upon electron addition to molecule of the halide, especially the stability of primary radical anion and pathways of its further transformations, depend on fine balance between thermodynamic parameters of the halide and products of its transformation.<sup>24,25</sup> In order to clarify the sequence of  $CHCl_3$  and R113 reduction reactions (in particular, to determine which group of R113 loses  $Cl^-$  first), quantum chemical studies of species which can potentially occur in these reactions were provided.

Geometry optimization of organic molecules was provided with triple- $\zeta$  valence basis set using DFT (with semiempirical correction for Van der Waals interactions) and SCS-MP2 (spin-component scaled second order Møller-Plesset perturbation

theory<sup>26</sup>) independently.

Exchange-correlation potential TPSS<sup>27</sup> which belongs to the most profound class of non-hybrid potentials (meta-GGA) was used for DFT. Usage of non-hybrid potential allowed to speed up the calculations efficiently with virtually no loss of accuracy via the resolution of identity approach.<sup>28</sup> Usage of hybrid potentials would require far larger computational efforts with no significant reduction of errors in geometry parameters.<sup>27,29</sup> However, meta-GGA potentials yield lesser errors compared to simpler GGA potentials which do not include expressions with laplacian of electronic density,<sup>27,29</sup> but the difference in the computational efforts is low.

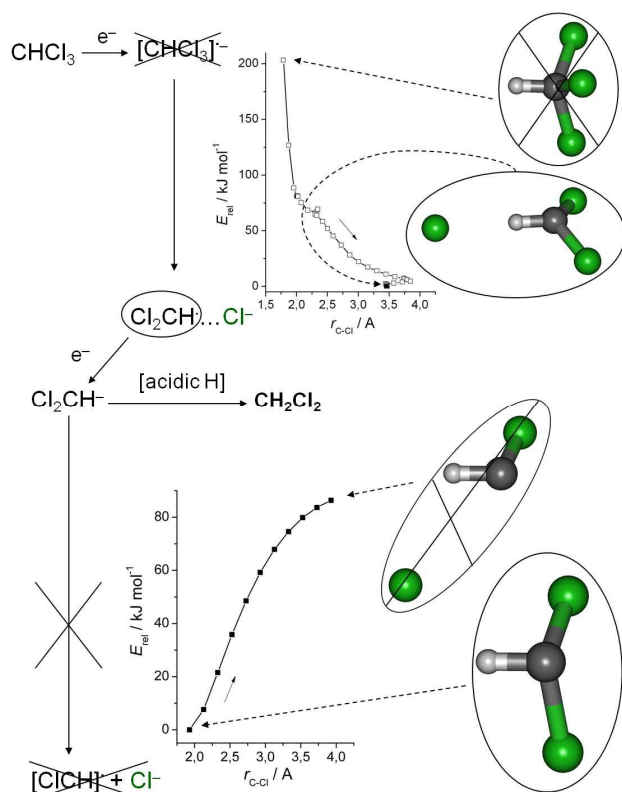
SCS-MP2 was used as an alternative wavefunction-based method with direct electron correlation treatment within perturbation theory. More profound treatment of electron correlation with geometry optimization (e.g. with CCSD(T) method) would require tremendous computational efforts. At the same time, application of semiempirical scaling coefficients in SCS-MP2 method allows to reach better results compared to non-scaled MP2 method.<sup>26</sup>

Geometry optimization of R113 molecule by DFT and SCS-MP2 methods yields the following bond length values:  $d(C-F) = 134-136$  pm (DFT) and  $133-135$  pm (SCS-MP2);  $d(C-Cl) = 178$  pm (DFT) and  $176$  pm (SCS-MP2),  $d(C-C) = 157$  pm (DFT) and  $156$  pm (SCS-MP2). Valent angles' values obtained by both methods lie in  $107-111^\circ$  range. Similarly,  $d(C-Cl)$  in  $CHCl_3$  is equal to  $179$  pm (DFT) and  $177$  pm (SCS-MP2),  $d(C-H) = 108$  pm (DFT and SCS-MP2), valent angles' values lie in  $108-111^\circ$  range. Experimentally found for  $CHCl_3$  in gas phase:  $d(C-Cl) = 177$  pm,  $d(C-H) = 107$  pm,  $Cl-C-Cl$  angle was equal to  $110.24^\circ$ ,<sup>30</sup> which was consistent with results of the calculations and may evidence in favor of correctness of these and the following calculations.

Geometry optimization by DFT of probable product of  $CHCl_3$  one-electron reduction – radical anion  $[CHCl_3]^-$  – showed, that such species was unstable. Equilibrium point of  $[CHCl_3]^-$  corresponded to barrier-less separation of one  $Cl^-$  ion along with formation of hydrogen bond  $H \dots Cl$  (Scheme 2). Clearly, the “step” on  $E$  vs  $r$  curve, preceding this equilibrium point, has no physical sense and represents a pathway chosen by geometry optimizer in order to locate the energy minimum. Hereinafter assignment of  $Cl$  to chloride ion (rather than  $Cl^\bullet$  radical) was confirmed by analysis of atomic charges and spin densities by a few different methods (Mulliken : charge  $-0.94$ , spin density  $0.0008$ ; ChelpG:31 charge  $-0.96$ ; Hirshfeld:32 charge  $-0.87$ , spin density  $0.002$ ; Becke:33 charge  $-0.96$ , spin density  $0.003$ ). Similar data were obtained using SCS-MP2 method.

DFT calculation showed, that product of the further reduction of  $[CHCl_2]^\bullet$  ( $[CHCl_2]^-$  anion) did not decompose, increase of  $C-Cl$  distance from  $1.928$  Å (equilibrium value for  $[CHCl_2]^-$ ) to  $3.928$  Å via relaxed surface scan (RSS) procedure with DFT (see Experimental section) led to electronic energy growth on  $90$  kJ/mol.‡

These findings are similar to the previously reported results of modeling of  $\text{CCl}_4$  molecule reduction in water.<sup>34</sup>



**Scheme 2** The stages of  $\text{CHCl}_3$  molecule reduction (the results of DFT modeling). Crossed systems were shown to be not stable. The open squares correspond to non-equilibrium steps of geometry relaxation, solid squares – to equilibrium geometries.

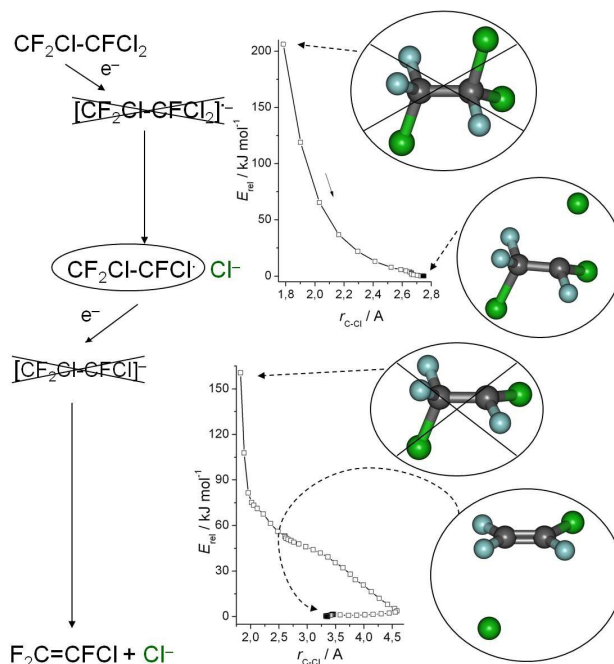
According to DFT calculations, the probable product of one-electron reduction of R113 – radical anion  $[\text{CF}_2\text{Cl}-\text{CFCl}_2]^\bullet-$  – was also unstable, the electronic energy minimum corresponded to separation of one chlorine anion (Mulliken atomic charge on leaving chlorine atom of  $\text{CF}_2\text{Cl}-\text{CFCl}_2$ :  $-0.81$ , spin density:  $0.17$ , ChelpG charge:  $-0.82$ ;

Hirshfeld: charge  $-0.76$ , spin density  $0.19$ ; Becke: charge  $-0.83$ , spin density  $0.19$ ) originated from  $-\text{CCl}_2\text{F}$  group (Scheme 3). The separation of chlorine anion from this group was probably facilitated by formation of resonance forms involving orbitals of the second Cl atom that belongs to this fragment. (Fig. 2). Distance from one of Cl atoms to C atom in  $[\text{CF}_2\text{Cl}-\text{CFCl}_2]^\bullet-$  increased to  $2.744 \text{ \AA}$  (DFT) or  $3.095 \text{ \AA}$  (SCS-MP2) compared to corresponding C–Cl separation in R113. These increased values a bit lesser than sum of Van der Waals radii of Cl and C ( $3.45 \text{ \AA}$ ),<sup>35</sup> but significantly exceeded the sum of their covalent radii ( $1.76 \text{ \AA}$ ).<sup>36</sup> It should be noted, that previously proposed mechanisms suggested that Cl atom of  $-\text{CF}_2\text{Cl}$  group eliminated first,<sup>20</sup> but no proofs of such suggestion were presented.

Analysis of electronic energy versus C–Cl distance for  $[\text{CF}_2\text{Cl}-\text{CFCl}_2]^\bullet-$  species by DFT method by RSS procedure showed, that increase of the distance ( $r$ ) to  $4.5 \text{ \AA}$  led to some energy ( $E$ ) growth ( $10 \text{ kJ/mol}$ ), followed by saturation of  $E$  vs.  $r$  curve. Similarly, SCS-MP2 RSS analysis showed energy oscillations within  $2\text{--}3 \text{ kJ/mol}$  range while increasing C–Cl distance (Fig. S1). So, both methods showed that there was some non-zero energy barrier of complete Cl– removing, but it was small enough and comparable with the energy of thermal motions of  $[\text{CF}_2\text{Cl}-\text{CFCl}]^\bullet$  radical.

Addition of electron to  $[\text{CF}_2\text{Cl}-\text{CFCl}]^\bullet$  radical (second stage

of two-electron reduction of R113) led to formation of  $[\text{CF}_2\text{Cl}-\text{CFCl}]^\bullet-$  anion (Scheme 3). Optimization of this anion by DFT showed, that it was also unstable, and the energy minimum corresponded to  $3.34 \text{ \AA}$  distance between C and Cl atoms of  $-\text{CF}_2\text{Cl}$  fragment (which is close to the sum of carbon and chlorine Van der Waals radii,  $3.45 \text{ \AA}$ ).<sup>35</sup> Such decomposition led to formation of trichlorofluoroethylene  $\text{CF}_2=\text{CFCl}$ . In contrast to DFT, SCS-MP2 calculation showed, that  $[\text{CF}_2\text{Cl}-\text{CFCl}]^\bullet-$  species did not decompose itself completely. However, energy barrier of increasing C–Cl distance within RSS procedure by  $0.2 \text{ \AA}$  was only  $10 \text{ kJ/mol}$ , and further separation of these atoms resulted in significant decrease of the energy (by  $100 \text{ kJ/mol}$  for  $3.6 \text{ \AA}$ , Fig. S2), so we can conclude from modeling by two methods that this anion is not stable.



**Scheme 3** The stages of R113 molecule reduction (the results of DFT modeling). Crossed systems were shown to be not stable. The open squares correspond to non-equilibrium steps of geometry relaxation, solid squares – to equilibrium geometries.

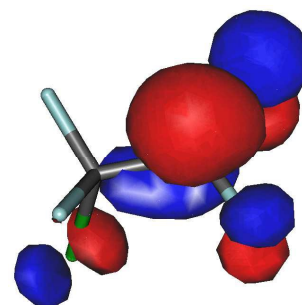


**Fig. 2** SOMO of  $[\text{CF}_2\text{Cl}-\text{CFCl}]^\bullet$  species.

These findings are similar to the previously reported results of modeling of  $\text{C}_2\text{Cl}_6$  molecule reduction in water.<sup>37</sup> On the other hand, in the contrary to previously reported cases,<sup>34,37</sup> where solvent influence was taken into account solely via implicit solvation, we provided additional investigation of  $\text{CHCl}_3$ ,

Cite this: DOI: 10.1039/c0xx00000x

www.rsc.org/xxxxxx

## ARTICLE TYPE

R113, [CHCl<sub>3</sub>]<sup>•-</sup>, [CHCl<sub>2</sub>]<sup>-</sup>, [R113]<sup>•-</sup> and [CF<sub>2</sub>Cl-CFCl]<sup>-</sup> with three explicit DMF molecules (these systems were also “put” into implicit solvent, see Experimental section for details). No specific interactions between solvent and substrate were observed in all these cases but some weak interactions (Mayer bond order 0.05 – 0.15; Fig. S3–S7) were found. This situation is quite similar to modeling of partially fluorinated methane and water solvent molecules,<sup>38</sup> however the bond orders, found in our case, were 2–3 times higher. It should be noted that addition of DMF molecules led to occurrence of small energy barrier (about 10 kJ/mol) for decomposition of [CF<sub>2</sub>Cl-CFCl]<sup>-</sup>, in contrast to DFT calculation of the same species within a model of implicit solvent. In any case, the energy of this barrier was comparable with the energy of thermal motions. It can be concluded that the results of modeling within the models of implicit solvent and the model of explicit solvent molecules are similar: both methods evidence for formation of the same intermediates and the same pathways of their transformations. Thus, the model of implicit solvent was used for further modeling of catalytic processes.

### Modeling of complexes reduction.

As it was reported by us,<sup>18,19</sup> the complex species M(L1)<sub>2</sub> (M<sup>II</sup> = Co, Ni, Fe) showed electrocatalytic activity in reductive electrochemical dehalogenation of organic halides (in particular, Ni(L1)<sub>2</sub> catalyzed dehalogenation of CHCl<sub>3</sub>, R113, BuI and CH<sub>2</sub>Br<sub>2</sub>; Co(L1)<sub>2</sub> and Fe(L1)<sub>2</sub> catalyzed dehalogenation of R113). M(L1)<sub>2</sub> complexes showed two reversible or quasi-reversible processes assigned to [M(L1)<sub>2</sub>]<sup>-</sup>/[M(L1)<sub>2</sub>]<sup>2-</sup> or [M(L1)<sub>2</sub>]<sup>0</sup>/[M(L1)<sub>2</sub>]<sup>-</sup> couples at E<sub>1/2</sub> in range -2.35 ÷ -2.20 V and -1.93 ÷ -1.65 V vs. Fc<sup>+</sup>/Fc couple, respectively.<sup>19</sup> The process [M(L1)<sub>2</sub>]<sup>0</sup>/[M(L1)<sub>2</sub>]<sup>-</sup> was responsible for catalytic activity in dehalogenation. In order to find where the additional electron is localized in [M(L1)<sub>2</sub>]<sup>-</sup> ions (*i.e.* the reduced forms of M(L1)<sub>2</sub>) quantum chemical modeling of [Co(L1)<sub>2</sub>], [Co(L1)<sub>2</sub>]<sup>-</sup>, [Ni(L1)<sub>2</sub>] and [Ni(L1)<sub>2</sub>]<sup>-</sup> species was carried out. Notably, the ligand L1H was also redox-active, and exhibited irreversible reduction at E<sub>c</sub> = -2.16 V vs. Fc<sup>+</sup>/Fc couple.<sup>19</sup>

Though X-ray molecular structure of neutral [Ni(L1)<sub>2</sub>]<sup>0</sup> molecule was determined, and [Co(L1)<sub>2</sub>]<sup>0</sup> was shown to be isostructural, a geometry optimization of these species using DFT method with exchange-correlation potential TPSS was carried in order to obtain geometries of these molecules taking solvation effects into account (details are presented in the Experimental section).

It can be concluded from comparison of ChelpG charge distributions and Mayer bond orders for [Co(L1)<sub>2</sub>]<sup>0</sup>, [Ni(L1)<sub>2</sub>]<sup>0</sup> and L1H (Tables 1 and 2), that coordination of CoII and NiII ions of L1<sup>-</sup> (*i.e.* replacement of H<sup>+</sup> into M<sup>2+</sup>) led to redistribution of electronic density in amide group: the electronic density increased at the nitrogen atom, almost didn't changed on the oxygen atom (despite its coordination) and decreased at the carbon atom. CO and CN bond orders (double and single in L1H, respectively) became almost equal (close to 1.5). Additionally,

electronic density on nitrogen atoms of azomethine and 2-pyridyl groups and the order of C=N bond (azomethine group) decreased in [Co(L1)<sub>2</sub>]<sup>0</sup> and [Ni(L1)<sub>2</sub>]<sup>0</sup> compared to L1H, which is consistent with coordination of these nitrogen atoms to the metal ions.

**Table 1** ChelpG charges on some atoms in L1H, [Co(L1)<sub>2</sub>]<sup>0</sup> and [Ni(L1)<sub>2</sub>]<sup>0</sup>.

| Atom           | L1H     | [Co(L1) <sub>2</sub> ] <sup>0</sup> | [Ni(L1) <sub>2</sub> ] <sup>0</sup> |
|----------------|---------|-------------------------------------|-------------------------------------|
| O (amide)      | -0.5742 | -0.5717; -0.5915                    | -0.5383; -0.5353                    |
| C (amide)      | 0.2716  | 0.5299; 0.5712                      | 0.5459; 0.5480                      |
| N (amide)      | 0.0021  | -0.7219; -0.7330                    | -0.7527; -0.7549                    |
| N (azomethine) | -0.3729 | 0.5105; 0.5143                      | 0.6330; 0.6427                      |
| C (azomethine) | -0.0729 | -0.4330; -0.4334                    | -0.5043; -0.5167                    |
| N (2-pyridyl)  | -0.7655 | -0.2586; -0.2645                    | -0.1817; -0.1836                    |
| N (4-pyridyl)  | -0.8178 | -0.7778; -0.7715                    | -0.7741; -0.7770                    |

Two different situations may occur upon addition of an electron to [Co(L1)<sub>2</sub>]<sup>0</sup> or [Ni(L1)<sub>2</sub>]<sup>0</sup> species (*i.e.* upon formation of [Co(L1)<sub>2</sub>]<sup>-</sup> and [Ni(L1)<sub>2</sub>]<sup>-</sup> anions). In the first case the electron occupies d-orbital of M<sup>II</sup> ion, hence, it is reduced to M<sup>I</sup> (case of “innocent” ligand). Multiplicity of [Co(L1)<sub>2</sub>]<sup>-</sup> anion, containing Co<sup>I</sup>, is 3 (2 in the case of [Ni(L1)<sub>2</sub>]<sup>-</sup>, containing Ni<sup>I</sup>). States with another multiplicities have energies with order of 10<sup>4</sup> cm<sup>-1</sup> higher.<sup>39</sup> In the second case the electron fully or partially occupies an antibonding orbital of L<sup>-</sup> ligand (case of “non-innocent” ligand). In this case two forms with different full spin values can exist (quintet and open-shell triplet for [Co(L1)<sub>2</sub>]<sup>-</sup> or quartet and open-shell doublet for [Ni(L1)<sub>2</sub>]<sup>-</sup>; the energy difference between the forms is small, order of tens or hundreds of cm<sup>-1</sup>).<sup>17</sup> The open-shell triplet form of [Co(L1)<sub>2</sub>]<sup>-</sup> (or open-shell doublet form of [Ni(L1)<sub>2</sub>]<sup>-</sup>), where additional electron is localized on L1<sup>-</sup>, can be considered as a complicated resonance structure consisting of forms with different combinations of orbitals filling.

Analysis of course and results of the DFT optimization of [Co(L1)<sub>2</sub>]<sup>-</sup> or [Ni(L1)<sub>2</sub>]<sup>-</sup> anions allows to reveal some indirect evidences that ligand is “non-innocent” in these cases. First, the self-consistent field of triplet (doublet) state of the complex shows signs of instability and tends to reach saddle points in optimization of the orbitals’ coefficients (comparing to the SCF of the high-spin quintet and quartet states, respectively, that converge easily using standard ORCA convergence accelerators). So, we failed to reach convergence tolerance ΔE = 10<sup>-8</sup> E<sub>h</sub> (desirable for gradients calculation) using DFT in SCF calculation for triplet form of [Co(L1)<sub>2</sub>]<sup>-</sup> species (as well as doublet [Ni(L1)<sub>2</sub>]<sup>-</sup>), but the optimization was continued with less strict tolerance, and self-consistency with 10<sup>-8</sup> E<sub>h</sub> tolerance was reached at the last steps of geometry optimization and yielded equilibrium energy -57.7 kJ/mol lower than the energy of the quintet state. For [Ni(L1)<sub>2</sub>]<sup>-</sup> the quartet state is 3.0 kJ/mol lower

than the doublet one. Comparison of energies for high spin, low spin and artificially constructed broken symmetry state (Table 3) may also show signs of resonance structure which corresponds to above mentioned “non-innocence”.<sup>40</sup> Also, spin contamination of low spin state indicates admixture of higher spin levels to the unrestricted SCF solution<sup>41</sup> which corresponds to the number of effectively unpaired electrons<sup>42,43</sup> that is a direct criterion of open shell character of the state (Table 3). Small differences in the above mentioned energies evidence for existence of low spin state with resonance structure (open-shell) that has an energy close to that of the appropriate high spin state. It also may be concluded from the comparison of the above mentioned energies and spin contaminations, that low spin state is more favored in the case of  $[\text{Co}(\text{L}1)_2]^-$  than in the case of  $[\text{Ni}(\text{L}1)_2]^-$ , and the electronic structure of the former is close to the regular triplet.

**Table 2** Mayer orders of bonds between some atoms in LH,  $[\text{Co}(\text{L}1)_2]^0$  and  $[\text{Ni}(\text{L}1)_2]^0$ .

| Bond                        | L1H    | $[\text{Co}(\text{L}1)_2]^0$ | $[\text{Ni}(\text{L}1)_2]^0$ |
|-----------------------------|--------|------------------------------|------------------------------|
| O(amide)–C(amide)           | 1.9733 | 1.4866; 1.4866               | 1.4904; 1.4912               |
| C(amide)–N(amide)           | 1.2617 | 1.5078; 1.5097               | 1.4669; 1.4682               |
| N(amide)–N(azomethine)      | 0.9310 | 0.9587; 0.9610               | 0.9721; 0.9711               |
| N(azomethine)–C(azomethine) | 1.8392 | 1.6469; 1.6336               | 1.6391; 1.6363               |

**Table 3** Parameters of different spin states of  $[\text{Co}(\text{L}1)_2]^-$  and  $[\text{Ni}(\text{L}1)_2]^-$ .<sup>a</sup>

|  | $[\text{Co}(\text{L}1)_2]^-$ | $[\text{Ni}(\text{L}1)_2]^-$ |
|--|------------------------------|------------------------------|
| High spin multiplicity                     | 5                            | 4                            |
| Low spin multiplicity                      | 3                            | 2                            |
| $E_{\text{HS}} - E_{\text{LS}}^b$ , kJ/mol | 57.7                         | -3.0                         |
| $E_{\text{HS}} - E_{\text{BS}}^c$ , kJ/mol | 32.0                         | -9.2                         |
| $E_{\text{HS}} - E_{\text{BS}}^d$ , kJ/mol | 129.4                        | -5.7                         |
| Spin contamination (LS) <sup>e</sup>       | 0.012                        | 0.752                        |

<sup>a</sup> “E” stands for electronic energy of a self-consistent state, namely: BS stands for the broken symmetry state obtained from converged high spin state by flipping one unpaired electron followed by self-consistency search, “HS” and “LS” stand for high spin and low spin states, respectively.

<sup>b</sup> at their equilibrium geometries

<sup>c</sup> at their equilibrium geometries at HS geometry, no COSMO,

<sup>d</sup> at LS geometry, no COSMO

<sup>e</sup> Deviation of found LS form  $\langle S^2 \rangle$  value from ideal value  $S(S+1)$  at LS geometry.

Thus, it can be concluded that high-spin and (open-shell) low-spin states in  $[\text{Ni}(\text{L}1)_2]^-$  have sufficiently close energies to be simultaneously occupied due to thermal distribution at room temperature. In general, correct spin state of the reduced form may be usually selected *a priori*, but  $[\text{M}(\text{L}1)_2]$  case demonstrates the compounds where such selection is not obvious. Analogous situation was reported previously for polyconjugated carbon materials.<sup>44</sup> Some prompts for appropriate selection can be derived from the analysis of electronic structure of the neutral forms of the complexes. “Additional” electron should occupy spin-up LUMO or spin-down LUMO of the species, so, the comparison of their energies (Table 4) can indicate more preferable multiplicity of the reduced state. Although DFT was

shown to be poor in prediction of ionization energies and electron affinities basing on HOMO and LUMO energies, the appropriate errors have a systematic character and may be canceled or compensated.<sup>45</sup> Thus, calculated energies of  $[\text{M}(\text{L}1)_2]$  ( $\text{M} = \text{Fe}, \text{Co}, \text{Ni}, \text{Zn}$ ) spin-up LUMOs are equal within 0.04 eV, while spin-down LUMOs’ energies vary from -3.0449 eV for  $[\text{Ni}(\text{L}1)_2]$  (which is 0.03 eV higher than appropriate spin-up one) to -3.9056 eV for  $[\text{Cu}(\text{L}1)_2]$  (which is 0.86 eV lower than appropriate spin-up one). This dependence agrees with above discussed results of detailed modeling of  $[\text{Ni}(\text{L}1)_2]^-$  and  $[\text{Co}(\text{L}1)_2]^-$  species: lower spin-down LUMO energy in respect to spin-up one favors low-spin state of the reduced form. The energies of spin-down LUMO correlate with  $E_{1/2}$  potentials of the  $[\text{M}(\text{L}1)_2]^0/[\text{M}(\text{L}1)_2]^-$  (Table 4)<sup>19</sup> and spin-down LUMO population on the metal atom (lower spin-down LUMO energy is associated with increasing of  $E_{1/2}$  and more localized character of the orbital, see also Fig. 3). We would like to note that there can be some contribution of surface-solution electron transfer effects in  $E_{1/2}$  values, determined in cyclic voltammetry experiment, but in the case of  $\text{M}(\text{L}1)_2$  complexes these effects (if any) should be minor or provide systematic shift of potentials for all metals (detailed discussion of this issue is presented in SI).

Thus, reduction of  $[\text{M}(\text{L}1)_2]_0$  complexes results in some change of geometry and electronic structure of the  $\text{M}(\text{L}1)_2$  unit, however we compared spin-down LUMOs of  $[\text{Ni}(\text{L}1)_2]_0$  and  $[\text{Co}(\text{L}1)_2]_0$  with corresponding orbitals in their reduced forms and found (quite expectedly) that these orbitals were almost identical. It can be concluded that an “additional” electron in  $[\text{M}(\text{L}1)_2]^-$  complexes ( $\text{M} = \text{Fe}, \text{Co}, \text{Ni}, \text{Cu}, \text{Zn}$ ) occupies the orbital, the nature of which gradually changes from mainly ligand-centered in  $[\text{Zn}(\text{L}1)_2]$  and  $[\text{Ni}(\text{L}1)_2]$  to mainly metal-centered in  $[\text{Cu}(\text{L}1)_2]$  and  $[\text{Co}(\text{L}1)_2]$ , while it was ambiguous in the case of  $[\text{Fe}(\text{L}1)_2]$ .

In order to check, if the situation with spin pseudodegeneracy of reduced catalytic species is typical, modeling of reduces forms of two other complexes was performed – (i) nickel complex with L2, i.e. reduced form of  $[\text{Ni}^{\text{II}}(\text{L}2)]$ , and (ii) a fragment of coordination polymer, cobalt complex with dithioamide of 1,3-benzenedicarboxylic acid (L3), i.e. reduced form of  $[\text{Co}^{\text{II}}\text{Cl}_2(\text{L}3)]_n$ . For the latter case a model species  $[\text{CoCl}_2(\text{L}3)]_2$  was used (see details in Experimental section). The choice of these systems was governed by high importance of  $[\text{Ni}^{\text{II}}(\text{L}2)]$  as electrocatalyst of dehalogenation of organic compounds,<sup>20</sup> and by the wish to study the influence of donor atom type (S compared to N and O) on distribution of electronic density upon one electron addition.

Cite this: DOI: 10.1039/c0xx00000x

www.rsc.org/xxxxxx

## ARTICLE TYPE

**Table 4** Energies of spin-up and spin-down LUMO orbitals.

| Compound                               | Spin-up LUMO energy, eV | Spin-down LUMO energy, eV | $E_{1/2}$ vs. $Fc^+/Fc$ , V               | Spin-down LUMO population on metal, % <sup>a</sup> |      |      |
|--|-------------------------|---------------------------|---|--|------|------|
| [Zn(L1) <sub>2</sub> ]                 | -3.0755                 | -3.0755                   | -1.93 <sup>19</sup>                       | 1.6  | 1.8  | 2.5  |
| [Ni(L1) <sub>2</sub> ]                 | -3.0725                 | -3.0449                   | -1.87 <sup>19</sup>                       | 6.2  | 7.0  | 7.5  |
| [Fe(L1) <sub>2</sub> ]                 | -3.1081                 | -3.3755                   | -1.70 <sup>19</sup>                       | 23.7   | 23.0 | 25.3 |
| [Co(L1) <sub>2</sub> ]                 | -3.0771                 | -3.5353                   | -1.65 <sup>19</sup>                       | 61.2   | 57.9 | 60.6 |
| [Cu(L1) <sub>2</sub> ]                 | -3.1090                 | -3.9056                   | -1.13 <sup>b</sup> 19                     | 56.3   | 56.9 | 59.4 |
| [Ni(L2) <sub>2</sub> ]                 | -2.5597                 | -2.5597                   | -2.02 <sup>46</sup><br>-2.15 <sup>c</sup> | 55.5   | 57.1 | 58.8 |
| [Co(L3) <sub>2</sub> Cl <sub>2</sub> ] | -3.0054                 | -3.7633                   | irreversible <sup>d</sup>                 | 62.8   | 60.5 | 62.4 |

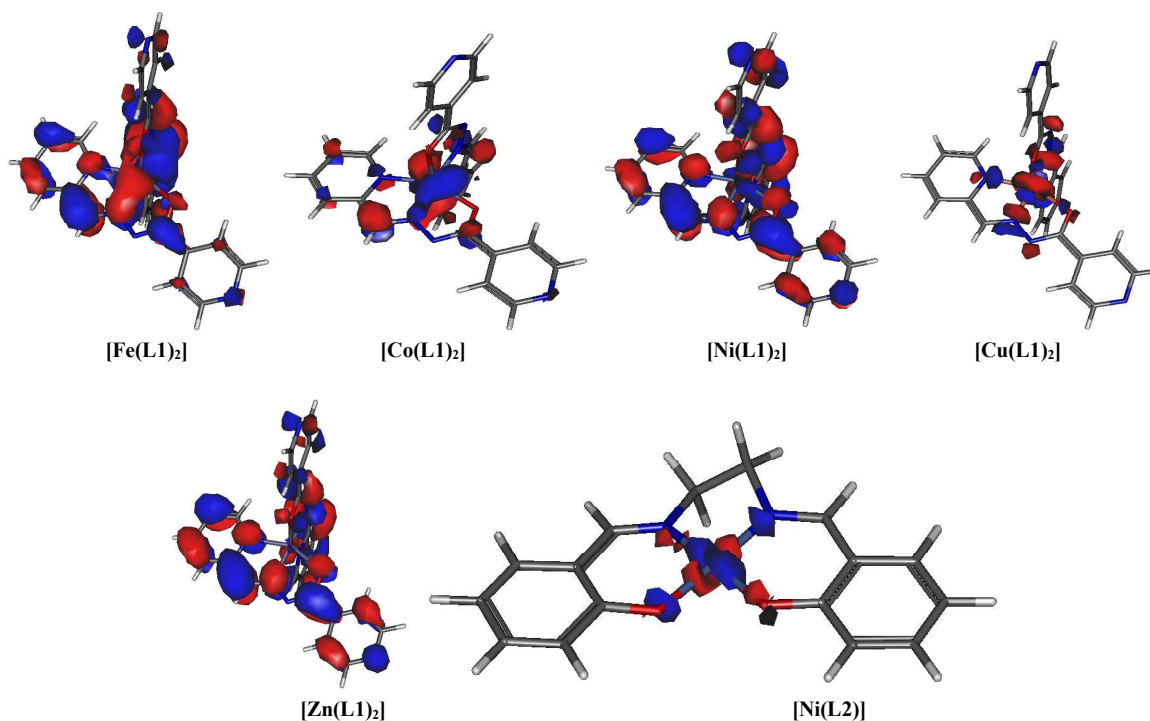
<sup>a</sup> First column in this section represents results of orbital composition analysis by Mulliken, Hirshfeld and Becke, respectively.

<sup>b</sup> Quasi-reversible.

<sup>c</sup> Our data, GC electrode, 0.1 M Et<sub>4</sub>NBF<sub>4</sub> in DMF.

<sup>d</sup>  $E_c = 1.16$  V measured for the [Co(L3)Cl<sub>2</sub>]<sub>n</sub> coordination polymer; our data, rough Pt plate electrode, 0.1 M Et<sub>4</sub>NBF<sub>4</sub> in MeCN (see Supplementary Info)

[Ni(L2)]<sup>0</sup> is a singlet species with low-spin Ni<sup>II</sup> ion in planar coordination sphere.<sup>47</sup> Thus, spin-up and spin-down LUMOs of [Ni(L2)]<sup>0</sup> are identical by shape and energy; [Ni(L2)]<sup>-</sup> has doublet multiplicity. The spin-down LUMO of [Ni(L2)]<sup>0</sup> was found to have metal-centered nature (Fig. 3 and Table 4). It can be concluded that delocalization of spin density in [M(L1)<sub>2</sub>]<sup>-</sup> species, described above, is not common case for metal complexes. However, the influence of electronic structure of metal complex (in particular, localization of "additional electron" in reduced species) on its electrocatalytic activity seems to be minor, if any, since both Ni(L1)<sub>2</sub> and Ni(L2) catalyze reduction of halides (*vide supra*).

**Fig. 3** Spin-down LUMO plots.

Cite this: DOI: 10.1039/c0xx00000x

www.rsc.org/xxxxxx

## ARTICLE TYPE

The initial geometry of  $[\text{CoCl}_2(\text{L}3)_2]^0$  was taken from crystallographic data in order to represent the geometry of the species within  $[\text{CoCl}_2(\text{L}3)]_n$  coordination polymer and the positions of all atoms except hydrogens were fixed in the optimization. Comparison of spin-up and spin-down LUMO energies of  $[\text{CoCl}_2(\text{L}3)_2]^0$  showed that spin-down one was significantly lower and was metal-centered (Table 4). So, triplet multiplicity was adopted for  $[\text{CoCl}_2(\text{L}3)_2]^-$  (Fig. 4).

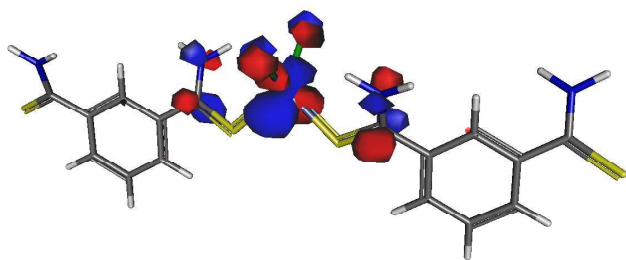


Fig. 4 The orbital that accepted additional electron in  $[\text{CoCl}_2(\text{L}3)_2]^-$  species, 75% isosurface.

Similarly to the case of L1H, ligand L2 is redox-active and shows irreversible reduction at  $E_c = -2.22$  V vs.  $\text{Fc}^+/\text{Fc}$  couple (on GC electrode in DMSO).<sup>48</sup> (which is close to redox-potential for  $[\text{Ni}(\text{L}2)]^{0/-}$  couple,  $E_{1/2} = -2.02$  V<sup>46</sup>), however, in contrast to the case of  $\text{Ni}(\text{L}1)_2$ , "additional" electron in the ion  $[\text{Ni}(\text{L}2)]^-$  is localized on metal ion. Similarly, both L3 and  $[\text{CoCl}_2(\text{L}3)_2]$  are redox-active ( $E_c = -1.95$  V for L3 vs.  $E_c = -1.16$  V for  $[\text{Co}(\text{L}3)\text{Cl}_2]_n$ ), but their direct comparison is not straightforward because of irreversible nature of redox-processes found in these cases. We can note, that redox-activity of ligand does not imply ligand-based reduction of its metal complex, and localization of "additional" electron is governed by LUMO nature rather than redox-activity of ligand or metal separately.

### Modeling of electron transfer from reduced complexes to halides

As it was previously shown by us,<sup>18,19</sup>  $\text{M}(\text{L}1)_2$  complexes exhibited electrocatalytic activity in reactions of organic halides dehalogenation, as it can be concluded from the increase of cathodic current (catalytic current) at potential, corresponding to  $[\text{M}(\text{L}1)_2]_0/[\text{M}(\text{L}1)_2]^-$  process, on cyclic voltammograms of DMF solutions, containing  $\text{M}(\text{L}1)_2$  complex, upon addition of halide.

It was found that electrocatalytic activity of  $\text{Co}(\text{L}1)_2$  and  $\text{Fe}(\text{L}1)_2$  was quite moderate: increase of R113 concentration led to current values saturation at the level about 50 % increase.<sup>19</sup> However, reduction of  $\text{CHCl}_3$  was not catalyzed by Co and Fe complexes. On the contrary,  $\text{Ni}(\text{L}1)_2$  catalyzed the reduction of both freon R113 and  $\text{CHCl}_3$ , and also catalyzed reduction of  $\text{CH}_2\text{Br}_2$  and *n*-C4H9I (two latter halides possessed much lower reduction potentials compared to R113 and  $\text{CHCl}_3$ ).<sup>18</sup> In the case of R113 reduction catalyzed by  $\text{Ni}(\text{L}1)_2$  at least 400 %

current growth was observed, but saturation was not achieved. In turn,  $\text{Zn}(\text{L}1)_2$  did not catalyze reduction of both R113 and  $\text{CHCl}_3$ , the appropriate current values were equal to the superposition of currents of  $\text{Zn}(\text{L}1)_2$  reduction and non-catalytic reduction of halide.<sup>19</sup> In order to verify if  $\text{Zn}(\text{L}1)_2$  can catalyze any organic halide reduction at all, we provided additional experiment (see SI, text and Fig. S8) and found that  $\text{Zn}(\text{L}1)_2$  catalyzed reduction of *n*-C4H9I. So, the absence of catalytic effect of  $\text{Zn}(\text{L}1)_2$  in the case of R113 and  $\text{CHCl}_3$  can be caused by too negative potential of  $\text{Zn}(\text{L}1)_2$ , in other words, molecules of the halides successfully "compete" with  $\text{Zn}(\text{L}1)_2$  for electrons from the electrode.

Thus, the activity of  $\text{M}(\text{L}1)_2$  complexes in reactions of halides dehalogenation strongly depended on the nature of the metal ion. This tendency is generally consistent with the difference between the potential of the mediator's redox-process and the potential of non-catalytic substrate reduction, which is typical for out-of-sphere electron transfer mechanism.<sup>49</sup> Also, no specific interactions between metal-containing compound and organic halide were observed while DFT geometry optimization of  $\{[\text{M}(\text{L}1)_2] \cdot \text{R}113\}^-$  ( $\text{M} = \text{Co}, \text{Fe}, \text{Ni}, \text{Zn}$ ) species (reductive decomposition of R113 in this adduct is considered below). These results indicate that  $[\text{M}(\text{L}1)_2]$  complexes act solely like electron transfer mediators rather than chemical catalysts, similarly to reported organic mediators.<sup>49</sup>

Modeling of electron transfer from  $[\text{M}(\text{L}1)_2]^-$  to R113 molecule was performed by a relaxed surface scanning of the energy of  $\{[\text{M}(\text{L}1)_2] \cdot \text{R}113\}^-$  adduct vs. C–Cl distance  $r_{\text{C-Cl}}$  (Fig. 5). Chlorine atom for RSS scan was selected on the grounds of modeling of  $[\text{R}113]^-$  decomposition, described above. In all studied cases, the system overcame moderate energy barrier (ca. 30 kJ/mol), followed by energy decay. The dependence of Becke atomic charges of the Cl atom (Fig. 5) showed distinct inflection near 2.4 Å (maximum of spin densities of the Cl atom vs  $r_{\text{C-Cl}}$  was approximately at the same point). In the case of  $\{[\text{Ni}(\text{L}1)_2] \cdot \text{R}113\}^-$  adduct distance value 2.59 Å corresponds to the values of charge  $-0.83$  and spin density 0.28. These findings evidence that energy maxima at  $r_{\text{C-Cl}}$  ca. 2.2 Å correspond to transition states in the reactions of catalytic reduction of R113 – formation of the adduct  $\{[\text{M}(\text{L}1)_2] \cdot [\text{CF}_2\text{Cl}-\text{CFCl}]\}^-$  and  $\text{Cl}^-$  anion. Sudden additional energy fall near  $r_{\text{C-Cl}} = 2.6\text{--}3.0$  Å was associated with conformation change of 4-pyridine ring of the complex. Different location of abrupt energy fall, associated with the conformation change, on energy profiles of the species was probably caused by small differences in their geometries. Further growth was probably caused by transformations of the Van der Waals adducts formed by disruption of C–Cl bond.

No significant difference in the RSS energy profiles was observed between high-spin  $\{[\text{Ni}(\text{L}1)_2] \cdot \text{R}113\}^-$  and low-spin  $\{[\text{Co}(\text{L}1)_2] \cdot \text{R}113\}^-$ . At the same time high-spin  $\{[\text{Co}(\text{L}1)_2] \cdot \text{R}113\}^-$  profile differed from the low-spin profile only by systematically higher energy of all its points, which is consistent with the difference between energies of HS and LS

forms of the species: ( $\{[\text{Co}(\text{L}1)_2]\cdot\text{R}113\}^-$  at small  $r_{\text{C-Cl}}$  and  $\{[\text{Co}(\text{L}1)_2]\cdot[\text{CF}_2\text{Cl}-\text{CFCl}]\cdot$  at large  $r_{\text{C-Cl}}$  (total spin of the system is preserved upon formation of  $\text{Cl}^-$  anion and  $\{[\text{Co}(\text{L}1)_2]\cdot[\text{CF}_2\text{Cl}-\text{CFCl}]\cdot$  adduct, containing  $\text{CF}_2\text{Cl}-\text{CFCl}\cdot$  radical).

In contrast to situation with  $\text{M}(\text{L}1)_2$  species, inner-sphere mechanism was proposed for electrocatalytic reduction of halides catalyzed by complexes of 3d metals with ligands of salen (L2) and porphyrin type.<sup>7,50</sup> This mechanism involved coordination of dechlorination intermediates to the axial positions of the metal ion in these complexes through C atom. <sup>7,51</sup> Current growth in the processes of R113 reduction catalyzed by  $\text{Ni}(\text{L}2)$  was at least 600 %, <sup>20</sup> and at least 900 % for  $\text{Co}(\text{L}2)$ .<sup>7</sup>

To study possible pathway of dehalogenation at presence of  $[\text{Ni}(\text{L}2)]^-$  we performed modeling of  $\{[\text{Ni}(\text{L}2)\cdot\text{R}113]\cdot$  species. Surprisingly, geometry optimization of this adduct led to direct barrier-less decomposition of the species and formation of  $[\text{NiIII}(\text{L}2)]\text{Cl}$ ,  $\text{CF}_2=\text{CFCl}$  and  $\text{Cl}^-$  without Ni-C bond formation (Fig. 6).

The absence and of barrier in the case of electron transfer within  $\{[\text{Ni}(\text{L}2)\cdot\text{R}113]\cdot$  species along with the presence of barrier in the case of electron transfer within  $\{[\text{M}(\text{L}1)_2]\cdot\text{R}113\}^-$  ( $\text{M} = \text{Ni}, \text{Co}$ ) species was consistent with higher catalytic activity of the former.

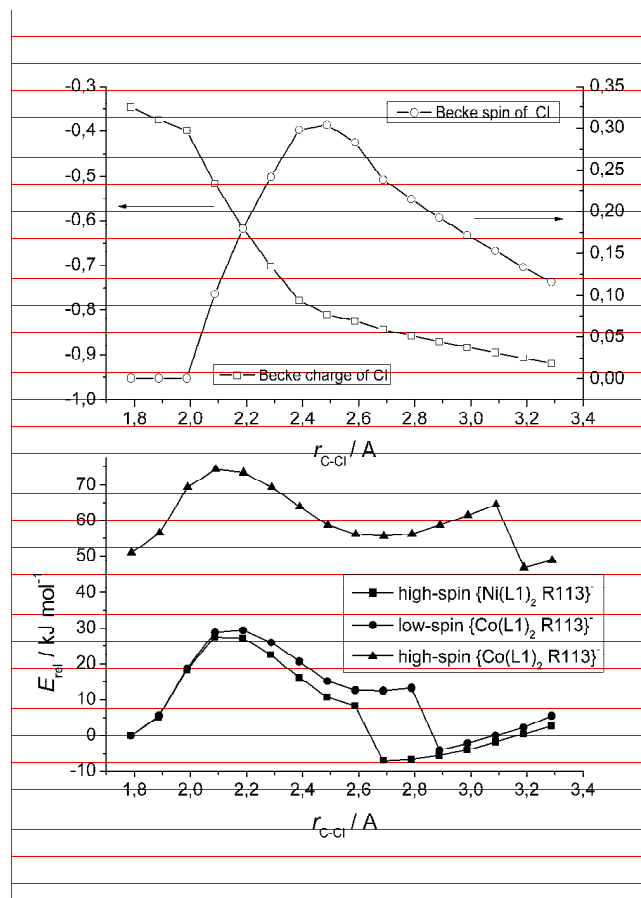


**Fig. 5** Results of relaxed surface scan of  $\{[\text{M}(\text{L}1)_2]\cdot\text{R}113\}^-$  adducts vs. C-Cl distance  $r_{\text{C-Cl}}$ . The curve for Ni-containing species was normalized on the energy of  $\{[\text{Ni}(\text{L}1)_2]\cdot\text{R}113\}^-$  (compound in the first point of the curve), while the curves for LS and HS forms of Co-

containing species were normalized on the energy of LS  $\{[\text{Co}(\text{L}1)_2]\cdot\text{R}113\}^-$ . Upper part of the figure shows change of Becke charge and spin density of Cl atom eliminating from R113 vs.  $r_{\text{C-Cl}}$  in  $\{[\text{Ni}(\text{L}1)_2]\cdot\text{R}113\}^-$ .

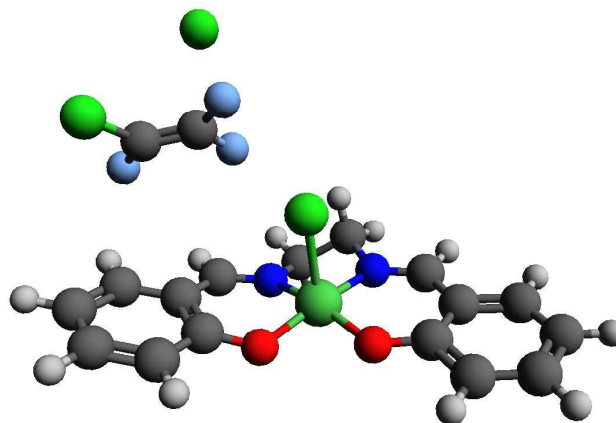


**Fig. 6** Equilibrium geometry of  $\{[\text{Ni}(\text{L}2)\cdot\text{R}113]\cdot$  species.

## Experimental section

### General remarks

All quantum chemical calculations were performed using ORCA software, versions 2.9.1 – 3.0.2.<sup>52</sup>

All molecular mechanics optimizations were performed using Avogadro software<sup>53</sup> with Universal force field (UFF).<sup>54</sup>

### Solvation

Unless explicitly mentioned, the calculations were performed for finite solvated species. Solvation effects were taken into account with COSMO (CONductor-like Screening MOdel).<sup>55</sup> DMF as a solvent with COSMO parameters built-in in ORCA unless explicitly mentioned.

### DFT

DFT calculations were performed using built-in def2-SVP and def2-TZVP<sup>56,57</sup> basis sets together with the corresponding built-in auxiliary basis sets (def2-SVP/J, def2-TZVP/J<sup>58</sup>) for Coulomb fitting within RI (resolution of identity) approximation, as implemented in ORCA.<sup>28</sup> TPSS exchange-correlation potential<sup>27</sup> was used. Van der Waals interactions were taken into account with Grimme DFT-D3 v.2.1 semiempirical correction<sup>59</sup> with Becke-Johnson damping<sup>60</sup> or without it.

### SCS-MP2

SCS-MP2 (spin component scaled second-order Møller-Plesset perturbation theory)<sup>26</sup> calculations were performed using built-in def2-TZVPP basis set, together with the corresponding built-in def2-TZVPP/J and def2-TZVPP/C auxiliary basis sets for RIJCOSX approximation.<sup>61</sup>

### Population analysis

Atomic charges, spin densities and orbital compositions were obtained using Mulliken62 and ChelpG31 (charges only) population analyses was used as implemented in ORCA as well as by population analyses based on Hirshfeld32 and Becke33

density partitioning schemes as implemented in Multiwfn 3.3.5 software.<sup>63,64</sup>

### Geometry optimizations

Geometry optimizations were performed in redundant internal coordinates with the following convergence tolerances (enforced by „TightOpt“ option): energy change –  $1e-6 E_h$ , RMS gradient –  $3e-5 E_h/\text{bohr}$ , max component of the gradient –  $1e-4 E_h/\text{bohr}$ , RMS step –  $6e-4 \text{ bohr}$ , max step –  $1e-3 \text{ bohr}$ .

The last cycle of geometry optimization of a species was used as the single point calculation at equilibrium geometries for this species.

### RSS (relaxed surface scan)

Relaxed surface scan procedure is a set of subsequent geometry optimizations, in which one internal coordinate (e.g. distance between two atoms) is consequently changed from equilibrium value to some value of interest with enough small step, while all other parameters are optimized at each value of the above mentioned scanned internal coordinate.

### Geometry optimizations of L1H; R113, CHCl<sub>3</sub>, CHCl<sub>3</sub>·3DMF, R113·3DMF and their reduction products.

Geometry optimization of L1H and CHCl<sub>3</sub>·3DMF was performed using DFT method; R113, CHCl<sub>3</sub> and their reduction products – using DFT and SCS-MP2 methods.

Only def2-SVP basis was used for CHCl<sub>3</sub>·3DMF and its reduced form, def2-TZVP was used for L1H, R113 and CHCl<sub>3</sub>. Also, def2-SVP basis was used for R113 and CHCl<sub>3</sub> in separate calculation to compare correctly the results of implicit and explicit solvent models, and such change of the basis did not lead to new effects.

Initial geometries for R113, CHCl<sub>3</sub>, CHCl<sub>3</sub>·3DMF, R113·3DMF and L1H were obtained using molecular mechanics method, charge of the molecules was set to 0, multiplicity – to 1. Initial geometries of R113, CHCl<sub>3</sub>, CHCl<sub>3</sub>·3DMF, R113·3DMF and L1H reduction products corresponded to equilibrium geometries of corresponding oxidized forms. For [CHCl<sub>3</sub>]<sup>•-</sup>, [CHCl<sub>3</sub>·3DMF]<sup>•-</sup>, [CF<sub>2</sub>Cl–CFCl]<sup>•-</sup>, [R113·3DMF]<sup>•-</sup> and [L1H]<sup>•-</sup> the charge was set to –1, multiplicity – to 2; for [CHCl<sub>2</sub>]<sup>•-</sup> and [CF<sub>2</sub>Cl–CFCl]<sup>•-</sup> (as well as [CHCl<sub>2</sub>·3DMF]<sup>•-</sup> and [CF<sub>2</sub>Cl–CFCl·3DMF]<sup>•-</sup>) – charge –1, multiplicity 1.

### [Co(L1)<sub>2</sub>]<sup>0</sup>, [Ni(L1)<sub>2</sub>]<sup>0</sup>, [Co(L1)<sub>2</sub>]<sup>-</sup> and [Ni(L1)<sub>2</sub>]<sup>-</sup> DFT calculation.

Initial geometries for oxidized forms ([Co(L1)<sub>2</sub>]<sup>0</sup> and [Ni(L1)<sub>2</sub>]<sup>0</sup>) were taken from crystallographic data for Fe(L1)<sub>2</sub> and Ni(L1)<sub>2</sub>, respectively. These geometries were preliminarily optimized with def2-SVP basis set (in order to save computational resources at the beginning of the optimization, when the geometry was far from equilibrium, and approximate calculation of electronic effects was sufficient), then the results were refined with def2-TZVP basis set. Magnetochemical data suggest that Co<sup>2+</sup> ion in [Co(L1)<sub>2</sub>]<sup>0</sup> is high-spin,<sup>19</sup> so, the multiplicity of [Co(L1)<sub>2</sub>]<sup>0</sup> species was set to 4, that corresponds to presence of 3 unpaired electrons on 3d orbitals of the Co<sup>2+</sup> ion.

The initial geometries for reduced forms ([Co(L1)<sub>2</sub>]<sup>-</sup> and [Ni(L1)<sub>2</sub>]<sup>-</sup>) were taken from results of def2-SVP optimizations and optimized with def2-SVP basis, then the results were refined with def2-TZVP basis.

### {[Ni(L1)<sub>2</sub>]<sup>-</sup>·R113}<sup>-</sup>, {[Fe(L1)<sub>2</sub>]<sup>-</sup>·R113}<sup>-</sup>, {[Co(L1)<sub>2</sub>]<sup>-</sup>·R113}<sup>-</sup>, {[Zn(L1)<sub>2</sub>]<sup>-</sup>·R113}<sup>-</sup> DFT calculation.

The initial geometries of the species were derived from the equilibrium high-spin geometries of the complexes and R113. The geometries of the particles were optimized with DFT using def2-SVP basis set and DFT-D version of semi-empirical Grimme correction for Van der Waals interactions.<sup>65</sup> The charge and geometry was set equal to appropriate pure high-spin complex species.

### Modeling of electron transfer (with R113 decomposition) in {[Ni(L1)<sub>2</sub>]<sup>-</sup>·R113}<sup>-</sup> and {[Co(L1)<sub>2</sub>]<sup>-</sup>·R113}<sup>-</sup>.

The initial geometries for these species (high-spin form of Ni one and both high-spin and low-spin forms for Co one) were obtained as described in the previous section. Then RSS scan along distance between carbon and one of the chlorine atoms (both C and Cl belong to –CFCl<sub>2</sub> group of R113) was performed on the same level of theory as for the initial geometry optimization.

### [Ni(L2)]<sup>0</sup> and [Ni(L2)]<sup>-</sup> DFT calculation.

The initial geometry for [Ni(L2)]<sup>0</sup> (charge 0, multiplicity 3) species was obtained using molecular mechanics optimization. Then it was optimized with DFT method with def2-SVP basis set, the result was then refined with def2-TZVP basis set.

The equilibrium geometry for [Ni(L2)]<sup>0</sup> was taken as the initial geometry for [Ni(L2)]<sup>-</sup>. The geometries of these anion species were optimized using DFT with def2-TZVP basis. The charges were set to –1, the multiplicities to 2.

### {[Ni(L2)]<sup>-</sup>·R113}<sup>-</sup> DFT calculation.

The initial geometry of the species was obtained using molecular mechanics optimization. Geometry optimization was provided in the same manner as for {[Ni(L1)<sub>2</sub>]<sup>-</sup>·R113}<sup>-</sup> (vide supra). Charge was set to –1 and multiplicity to 2.

### [CoCl<sub>2</sub>(L3)<sub>2</sub>]<sup>0</sup> and [CoCl<sub>2</sub>(L3)<sub>2</sub>]<sup>-</sup> DFT calculation.

The initial geometry for [CoCl<sub>2</sub>(L3)<sub>2</sub>]<sup>0</sup> was taken from crystallographic data for [CoCl<sub>2</sub>(L3)<sub>n</sub>] coordination polymer which had been previously reported by us.<sup>21</sup> Only positions of the hydrogen atoms were optimized using DFT method with def2-TZVP basis set (the positions of all other atoms were fixed during the optimization in order to reproduce the arrangement of ligands in a crystal of the coordination polymer). The equilibrium geometry of [CoCl<sub>2</sub>(L3)<sub>2</sub>]<sup>0</sup> was also used for single point calculation of [CoCl<sub>2</sub>(L3)<sub>2</sub>]<sup>-</sup>. Acetonitrile was used as the solvent for COSMO model (with parameters built-in in ORCA). In the case if this species was optimized without restrictions it collapsed due to  $\pi$ -stacking between L3 ligands, coordinated to one Co ion, which obviously did not represent its structure in real coordination polymer.

All potentials of electrochemical processes were referred to Fc<sup>+/0</sup>/Fc (Fc = ferrocene) couple potentials using reference electrodes descriptions presented in the correspondent papers and potentials of standard electrodes reported earlier.<sup>66</sup>

## Conclusions

In this study the processes, which occur upon electrochemical reduction of organic halides and metal complexes – electrocatalysts of such processes – were modeled.

It was shown by DFT and SCS-MP2 methods that one electron accepting by CHCl<sub>3</sub> or R113 molecules led to formation of radical anions, that lost Cl<sup>-</sup> forming [CHCl<sub>2</sub>]<sup>•-</sup> or [CF<sub>2</sub>Cl–CFCl]<sup>•-</sup> (without a barrier or with small barrier, compared to the energy of

thermal motions at room temperature). After accepting of the second electron by  $[\text{CHCl}_2]^-$  a stable  $[\text{CHCl}_2]^-$  anion formed. In contrast, addition of the second electron to  $[\text{CF}_2\text{Cl}-\text{CFCl}]^+$  radical led to lost of the second  $\text{Cl}^-$  anion yielding  $\text{CF}_2=\text{CFCl}$ . Examination of these species ( $\text{CHCl}_3$ , R113 and intermediates of their reduction) within the model of implicit solvent or optimization of the adducts with explicit solvent molecules produced similar results; it can be concluded that the model of implicit solvent is adequate and thus it was used for modeling of metal-containing species and processes. Modeling of reductive dehalogenation of R113 revealed, that Cl atom from  $-\text{CFCl}_2$  group was eliminated first (in contrast to  $-\text{CF}_2\text{Cl}$ ), contradicting to previous suppositions.

It was shown by DFT method, that a series of  $[\text{M}(\text{L}1)_2]^0$  complexes ( $\text{M} = \text{Fe}, \text{Co}, \text{Ni}, \text{Cu}, \text{Zn}$ ), which possess very similar structures, exhibited different nature of electrochemical redox-processes  $[\text{M}(\text{L}1)_2]^0/[\text{M}(\text{L}1)_2]^-$ , gradually changing from mainly ligand-centered in  $[\text{Zn}(\text{L}1)_2]$  and  $[\text{Ni}(\text{L}1)_2]$  to mainly metal-centered in  $[\text{Cu}(\text{L}1)_2]$  and  $[\text{Co}(\text{L}1)_2]$ .  $[\text{Fe}(\text{L}1)_2]$  showed ambiguous nature of redox-transition. It was found that  $[\text{M}(\text{L}1)_2]^-$  species (except  $[\text{Zn}(\text{L}1)_2]^-$ ) could exist in two states that differ by the value of full spin; these states were studied in details for  $\text{M} = \text{Ni}$  or  $\text{Co}$  by DFT examination of their reduced forms in both spin states. Energy differences between these forms are small enough and both states can be thermally populated. Low-spin state is slightly higher by energy than high-spin one for  $[\text{Ni}(\text{L}1)_2]^-$  according to the results of DFT calculations, and remarkably lower for  $[\text{Co}(\text{L}1)_2]^-$ . However, the difference between energies of calculated spin-up (close for all complexes in the series) and spin-down LUMO (the latter is slightly higher than spin-up one for  $[\text{Ni}(\text{L}1)_2]$  and decreases in the series  $[\text{Ni}(\text{L}1)_2] > [\text{Fe}(\text{L}1)_2] > [\text{Co}(\text{L}1)_2] > [\text{Cu}(\text{L}1)_2]$ ) correlates with: (1) the relative energies of low-spin and high-spin states; (2) experimental  $E_{1/2}$  potentials of the appropriate redox-transitions; (3) nature (shape and contribution of the metal ion to the orbital) of the spin-down LUMO orbital.

In contrast to the  $[\text{Ni}(\text{L}1)_2]$  case, the process  $[\text{Ni}(\text{L}2)]^0/[\text{Ni}(\text{L}2)]^-$  was metal-centered. In order to see the influence of donor atoms in coordination sphere of metal ion on "additional" electron localization, anionic particle  $[\text{Co}(\text{L}3)_2\text{Cl}_2]^-$  was modeled, that represents electron addition to coordination polymer  $[\text{Co}(\text{L}3)\text{Cl}_2]_n$ . Reduction of  $[\text{Co}(\text{L}3)_2\text{Cl}_2]^0$  was found to be metal-centered and yielded anion with low-spin triplet state. Taking into account close values of  $E_c$  values of  $\text{H}_2\text{L}2$  and  $\text{L}1\text{H}$  reduction, as well as  $E_{1/2}$  for  $[\text{Ni}(\text{L}1)_2]^0/[\text{Ni}(\text{L}1)_2]^-$  and  $[\text{Ni}(\text{L}2)]^0/[\text{Ni}(\text{L}2)]^-$  transitions, no correlation between the nature of the process and electrochemical properties of the ligands was found in this case.

Examination of  $\{[\text{M}(\text{L}1)_2]\cdot\text{R}113\}^-$  ( $\text{M} = \text{Fe}, \text{Co}, \text{Ni}, \text{Zn}$ ) species revealed no specific influence of metal complex on electronic structure of the organic halide, which suggests outer-sphere electron transfer by  $\text{M}(\text{L}1)_2$  species rather than specific chemical catalysis by them. Electron transfer in  $\{[\text{M}(\text{L}1)_2]\cdot\text{R}113\}^-$  ( $\text{M} = \text{Ni}, \text{Co}$ ) adducts with elimination of Cl anion from R113 molecule was studied by relaxed surface scan vs. the C–Cl distance and was found to occur with energy barrier at the level ca. 30 kJ/mol. In contrast, decomposition of  $\{[\text{M}(\text{L}2)]\cdot\text{R}113\}^-$  adduct occurred without energy barrier. The

presence of energy barrier in the processes of  $\{[\text{catalyst}\cdot\text{R}113]\}^-$  adducts decomposition is consistent with the difference in catalytic activity of these complexes (in terms of catalytic current values).

On the grounds of comparison of catalytic activity of  $\text{Ni}(\text{L}1)_2$ ,  $\text{Co}(\text{L}1)_2$ ,  $\text{Fe}(\text{L}1)_2$  and  $\text{Ni}(\text{L}2)$  in reactions of R113 or  $\text{CHCl}_3$  reduction we can conclude that the nature of redox-process in metal complex has no influence on its ability to act as electrocatalyst. Redox-processes in the complexes of  $\text{M}(\text{L}1)_2$  series, which showed catalytic activity, were ligand-centered, mixed or metal-centered. In turn, catalytic activity expectedly depends on the difference between redox-potentials of the catalyst and substrate and the presence (height) of electron transfer energy in the adduct of reduced catalyst and substrate.

## Acknowledgements

The authors thank to V.E. Lashkaryov Institute of Semiconductor Physics NAS of Ukraine for granting their computational cluster resources and to Dr. Oleksiy V. Khavryuchenko for fruitful discussion. This work was partially supported by joint grant of the National Academy of Sciences of Ukraine and Russian Foundation for Basic Research (No. 03-03-14), Russian Foundation for Basic Research (No. 14-03-90423), Russian Academy of Sciences and the National Academy of Sciences of Ukraine, the Council on Grants of the President of the Russian Federation (grant NSH-4773.2014.3).

## Notes and references

<sup>a</sup> L. V. Piszarzhetskii Institute of Physical Chemistry of the National Academy of Sciences of the Ukraine, Prospekt Nauki 31, Kiev, 03028, Ukraine

\* Corresponding author. Fax +38 044 525 6216. E-mail: litvinkenkoas@mail.ru

<sup>b</sup> N. S. Kurnakov Institute of General and Inorganic Chemistry, Russian Academy of Sciences, Leninsky Prospect 31, 119991 Moscow, GSP-1, Russian Federation

† Electronic Supplementary Information (ESI) available: experimental details for cyclic voltammetry experiments, experimental CV plots of  $\text{Zn}(\text{L}1)_2$  and n-C4H9I solutions, SCS-MP2 energy profiles, equilibrium geometry plots of halide reduction intermediates with explicit DMF molecules with notable bond orders, selected protocols (output files) for quantum-chemical calculations. See DOI: 10.1039/b000000x/

‡ In solution  $\text{CHCl}_2^-$  anion accepts  $\text{H}^+$  from solvent or background electrolyte, but these processes are not rate-limiting steps of halide reduction and were not modeled by us.

1 A. Deronzier and J.-C. Moutet, in *Comprehensive Coordination Chemistry II*, eds. J. A. McCleverty and T. J. Meyer, Pergamon, Oxford, 2003, pp. 471–507.

2 A. L. Ward, L. Elbaz, J. B. Kerr and J. Arnold, *Inorg. Chem.*, 2012, **51**, 4694–4706.

3 M. Bourrez, F. Molton, S. Chardon-Noblat and A. Deronzier, *Angew. Chem.*, 2011, **123**, 10077–10080.

4 J. P. Collin, A. Jouaiti and J. P. Sauvage, *Inorg. Chem.*, 1988, **27**, 1986–1990.

5 E. E. Benson, C. P. Kubiak, A. J. Sathrum and J. M. Smieja, *Chem. Soc. Rev.*, 2008, **38**, 89–99.

6 M. L. Helm, M. P. Stewart, R. M. Bullock, M. R. DuBois and D. L. DuBois, *Science*, 2011, **333**, 863–866.

7 J. D. Persinger, J. L. Hayes, L. J. Klein, D. G. Peters, J. A. Karty and J. P. Reilly, *J. Electroanal. Chem.*, 2004, **568**, 157–165.

- 8 P. Vanalabhpatana and D. G. Peters, *Tetrahedron Lett.*, 2003, **44**, 3245–3247.
- 9 E. Dolhem, R. Barhdadi, J. C. Folest, J. Y. Nédelec and M. Troupel, *Tetrahedron*, 2001, **57**, 525–529.
- 5 10 M. Oçafraïn, M. Devaud, M. Troupel and J. Périchon, *J. Chem. Soc. Chem. Commun.*, 1995, 2331–2332.
- 11 V. E. Titov, A. M. Mishura and V. G. Koshechko, *Theor. Exp. Chem.*, 2011, **46**, 399–408.
- 12 R. A. Maithreepala and R. Doong, *Environ. Sci. Technol.*, 2005, **39**, 4082–4090.
- 10 13 V. G. Koshechko and V. D. Pokhodenko, *Theor. Exp. Chem.*, 1997, **33**, 230–247.
- 14 P. C. Gach, J. A. Karty and D. G. Peters, *J. Electroanal. Chem.*, 2008, **612**, 22–28.
- 15 15 B. K. Sweeny and D. G. Peters, *Electrochem. Commun.*, 2001, **3**, 712–715.
- 16 P. V. Bernhardt and L. A. Jones, *Inorg. Chem.*, 1999, **38**, 5086–5090.
- 17 W. Kaim, *Inorg. Chem.*, 2011, **50**, 9752–9765.
- 18 A. S. Lytvynenko, S. V. Kolotilov, M. A. Kiskin, O. Cador, S. Golhen, G. G. Aleksandrov, A. M. Mishura, V. E. Titov, L. Ouahab, I. L. Eremenko and V. M. Novotortsev, *Inorg. Chem.*, 2014, **53**, 4970–4979.
- 20 19 A. S. Lytvynenko, A. M. Mishura, V. E. Titov, M. A. Kiskin, S. Golhen, O. Cador, S. V. Kolotilov, L. Ouahab, I. L. Eremenko, V. M. Novotortsev, *Russ. Chem. Bull.*, submitted.
- 25 20 E. R. Wagoner, J. L. Hayes, J. A. Karty and D. G. Peters, *J. Electroanal. Chem.*, 2012, **676**, 6–12.
- 21 A. S. Lytvynenko, S. V. Kolotilov, O. Cador, S. Golhen, L. Ouahab and V. V. Pavlishchuk, *New J. Chem.*, 2011, **35**, 2179–2186.
- 30 22 E. R. Wagoner and D. G. Peters, *J. Electrochem. Soc.*, 2013, **160**, G135–G141.
- 23 *US Pat.*, 5 569 809, 1996.
- 24 L. Pause, M. Robert and J.-M. Savéant, *J. Am. Chem. Soc.*, 2000, **122**, 9829–9835.
- 35 25 C. Costentin, M. Robert and J.-M. Savéant, *Chem. Phys.*, 2006, **324**, 40–56.
- 26 S. Grimme, *J. Chem. Phys.*, 2003, **118**, 9095–9102.
- 27 J. Tao, J. P. Perdew, V. N. Staroverov and G. E. Scuseria, *Phys. Rev. Lett.*, 2003, **91**, 146401.
- 40 28 F. Neese, *J. Comput. Chem.*, 2003, **24**, 1740–1747.
- 29 M. Bühl and H. Kabrede, *J. Chem. Theory Comput.*, 2006, **2**, 1282–1290.
- 30 S. N. Ghosh, R. Trambarulo and W. Gordy, *J. Chem. Phys.*, 2004, **20**, 605–607.
- 45 31 C. M. Breneman and K. B. Wiberg, *J. Comput. Chem.*, 1990, **11**, 361–373.
- 32 F. L. Hirshfeld, *Theor. Chim. Acta*, 1977, **44**, 129–138.
- 33 A. D. Becke, *J. Chem. Phys.*, 1988, **88**, 2547–2553.
- 34 N. Zhang, P. Blowers and J. Farrell, *Environ. Sci. Technol.*, 2005, **39**, 612–617.
- 50 35 M. Mantina, A. C. Chamberlin, R. Valero, C. J. Cramer and D. G. Truhlar, *J. Phys. Chem. A*, 2009, **113**, 5806–5812.
- 36 P. Kurzweil and P. Scheipers, in *Chemie*, Vieweg+Teubner Verlag, 2012, pp. 31–43.
- 55 37 E. V. Patterson, C. J. Cramer and D. G. Truhlar, *J. Am. Chem. Soc.*, 2001, **123**, 2025–2031.
- 38 I. Alkorta, I. Rozas and J. Elguero, *J. Fluor. Chem.*, 2000, **101**, 233–238.
- 39 W. Kaim and B. Schwederski, *Pure Appl. Chem.*, 2004, **76**, 351–364.
- 60 40 V. Bachler, G. Olbrich, F. Neese and K. Wieghardt, *Inorg. Chem.*, 2002, **41**, 4179–4193.
- 41 D. C. Young, *Computational chemistry a practical guide for applying techniques to real world problems*, Wiley, New York, 2001.
- 42 V. N. Staroverov and E. R. Davidson, *Chem. Phys. Lett.*, 2000, **330**, 161–168.
- 65 43 I. Zilberberg and S. P. Ruzankin, *Chem. Phys. Lett.*, 2004, **394**, 165–170.
- 44 O. V. Khavryuchenko, V. D. Khavryuchenko and G. H. Peslherbe, *J. Phys. Chem. A*, 2014, **118**, 7052–7057.
- 70 45 G. Zhang and C. B. Musgrave, *J. Phys. Chem. A*, 2007, **111**, 1554–1561.
- 46 M. S. Mubarak, W. E. Barker and D. G. Peters, *J. Electrochem. Soc.*, 2007, **154**, F205.
- 47 J. A. McCleverty and T. J. Meyer, Eds., *Comprehensive coordination chemistry II: from biology to nanotechnology*, Elsevier Pergamon, Amsterdam; Boston, 1st ed., 2004.
- 75 48 S. Zolezzi, E. Spodine and A. Decinti, *Polyhedron*, 2002, **21**, 55–59.
- 49 V. E. Titov, P. B. Paramonov and V. G. Koshechko, *Theor. Exp. Chem.*, 2001, **37**, 92–97.
- 80 50 Y. Zhang, W. Shen, Z. Ou, W. Zhu, Y. Fang and K. M. Kadish, *Electroanalysis*, 2013, **25**, 1513–1518.
- 51 C. Gosden, K. P. Healy and D. Pletcher, *J. Chem. Soc. Dalton Trans.*, 1978, 972–976.
- 52 F. Neese, *Wiley Interdiscip. Rev. Comput. Mol. Sci.*, 2012, **2**, 73–78.
- 85 53 M. D. Hanwell, D. E. Curtis, D. C. Lonie, T. Vandermeersch, E. Zurek and G. R. Hutchison, *J. Cheminformatics*, 2012, **4**, 17.
- 54 A. K. Rappe, C. J. Casewit, K. S. Colwell, W. A. Goddard and W. M. Skiff, *J. Am. Chem. Soc.*, 1992, **114**, 10024–10035.
- 55 A. Klamt and G. Schüürmann, *J. Chem. Soc. Perkin Trans. 2*, 1993, 799–805.
- 90 56 F. Weigend and R. Ahlrichs, *Phys. Chem. Chem. Phys.*, 2005, **7**, 3297–3305.
- 57 A. Schäfer, H. Horn and R. Ahlrichs, *J. Chem. Phys.*, 1992, **97**, 2571.
- 58 F. Weigend, *Phys. Chem. Chem. Phys.*, 2006, **8**, 1057–1065.
- 95 59 S. Grimme, J. Antony, S. Ehrlich and H. Krieg, *J. Chem. Phys.*, 2010, **132**, 154104.
- 60 E. R. Johnson and A. D. Becke, *J. Chem. Phys.*, 2006, **124**, 174104.
- 61 F. Neese, F. Wennmohs, A. Hansen and U. Becker, *Chem. Phys.*, 2009, **356**, 98–109.
- 100 62 R. S. Mulliken, *J. Chem. Phys.*, 1955, **23**, 1833–1840.
- 63 T. Lu and F. Chen, *J. Comput. Chem.*, 2012, **33**, 580–592.
- 64 Tian Lu, Feiwu Chen, *Acta Chim. Sinica*, 2011, **69**, 2393–2406.
- 65 S. Grimme, *J. Comput. Chem.*, 2004, **25**, 1463–1473.
- 66 V. V. Pavlishchuk and A. W. Addison, *Inorganica Chim. Acta*, 2000, **298**, 97–102.